Received: 8 December 2017 | Revised: 15 April 2018 | Accepted: 17 April 2018

DOI: 10.1111/gcb.14324

PRIMARY RESEARCH ARTICLE

WILEY Global Change Biology

Geographical CO_2 sensitivity of phytoplankton correlates with ocean buffer capacity

Sophie Richier[1] | Eric P. Achterberg[1,2] | Matthew P. Humphreys[1,3] | Alex J. Poulton[4] | David J. Suggett[5,6] | Toby Tyrrell[1] | Christopher Mark Moore[1]

[1]Ocean and Earth Science, National Oceanography Centre Southampton, University of Southampton, Southampton, UK

[2]GEOMAR Helmholtz Centre for Ocean Research, Kiel, Germany

[3]Centre for Ocean and Atmospheric Sciences, School of Environmental Sciences, University of East Anglia, Norwich, UK

[4]National Oceanography Centre, Southampton, UK

[5]School of Biological Sciences, University of Essex, Essex, UK

[6]Climate Change Cluster (C3), University of Technology Sydney, Broadway, NSW, Australia

Correspondence
Sophie Richier, Centre d'Etude et de Valorisation des Algues (CEVA) Presqu'île de Pen Lan, 22610 Pleubian, France.
Email: sophie.richier@ceva.fr

Present address
Alex J. Poulton, The Lyell Centre, Heriot-Watt University, Edinburgh, UK.

Funding information
UK Ocean Acidification (UKOA) programme via Natural Environment Research Council, Grant/Award Number: NE/H017348/1, NE/H017097/1, NE/H017062/1; Australian Research Council Future Fellowship, Grant/Award Number: FT130100202

Abstract

Accumulation of anthropogenic CO_2 is significantly altering ocean chemistry. A range of biological impacts resulting from this oceanic CO_2 accumulation are emerging, however, the mechanisms responsible for observed differential susceptibility between organisms and across environmental settings remain obscure. A primary consequence of increased oceanic CO_2 uptake is a decrease in the carbonate system buffer capacity, which characterizes the system's chemical resilience to changes in CO_2, generating the potential for enhanced variability in pCO_2 and the concentration of carbonate [CO_3^{2-}], bicarbonate [HCO_3^-], and protons [H^+] in the future ocean. We conducted a meta-analysis of 17 shipboard manipulation experiments performed across three distinct geographical regions that encompassed a wide range of environmental conditions from European temperate seas to Arctic and Southern oceans. These data demonstrated a correlation between the magnitude of natural phytoplankton community biological responses to short-term CO_2 changes and variability in the local buffer capacity across ocean basin scales. Specifically, short-term suppression of small phytoplankton (<10 μm) net growth rates were consistently observed under enhanced pCO_2 within experiments performed in regions with higher ambient buffer capacity. The results further highlight the relevance of phytoplankton cell size for the impacts of enhanced pCO_2 in both the modern and future ocean. Specifically, cell size-related acclimation and adaptation to regional environmental variability, as characterized by buffer capacity, likely influences interactions between primary producers and carbonate chemistry over a range of spatio-temporal scales.

KEYWORDS
anthropogenic change, carbonate chemistry, carbonate system buffer capacity, cell size, experimental manipulation, ocean acidification

1 | INTRODUCTION

Phytoplankton play a pivotal role in marine ecosystems and ocean biogeochemistry, and hence have been the focus of intensive research into the potential for ongoing changes in marine carbonate chemistry driven by the continued uptake of anthropogenic atmospheric CO_2 (often termed ocean acidification, OA) (Doney, Fabry, Feely & Kleypas, 2009; Royal Society, 2005) to influence their physiology, ecology, and productivity. Phytoplankton have been demonstrated to display a variety of physiological sensitivities to OA within experimental manipulations performed over a range of timescales (Collins, Rost & Rynearson, 2014; Dutkeiwicz et al., 2015; Kroeker et al., 2013; Riebesell & Tortell, 2011; Riebesell et al., 2017; Wu, Campbell, Irwin, Suggett & Finkel, 2014). However, robust

reproducible responses and a clear mechanistic understanding of the observed differential responses have remained elusive (Bach, Riebesell, Gutowska, Federwisch & Schulz, 2015; Flynn et al., 2012; Kroeker et al., 2013).

In addition to altering the absolute concentrations of a range of chemical species, including pCO_2, carbonate [CO_3^{2-}], bicarbonate [HCO_3^-], and protons [H^+], OA also leads to decreases in the carbonate system buffer capacity (Egleston, Sabine & Morel, 2010; Frankignoulle, 1994). Carbonate chemistry system (CCS) variability as a result of both biotic and abiotic forcing is thus expected to increase in the future ocean (Egleston et al., 2010; Flynn et al., 2012). Moreover, these ongoing changes in carbonate chemistry are occurring against a background of both natural and anthropogenically altered gradients in a range of other potentially interacting environmental drivers of phytoplankton ecophysiology (Boyd, Lennartz, Glover & Doney, 2015; Boyd, Strzepek, Fu & Hutchins, 2010; Boyd et al., 2016), including temperature (Humphreys, 2017; Kroeker et al., 2013; Tatters, Roleda et al., 2013; Tatters, Schnetzer et al., 2013) and nutrient availability (Hoppe et al., 2013; Muller, Trull & Hallegraeff, 2017). Integrative understanding of how OA is likely to influence phytoplankton ecophysiology, and consequently ocean biogeochemistry, requires an appreciation of the potential for variability in a range of these environmental conditions to modulate responses (Boyd, 2011).

Within experimental studies, significant physiological responses to altered carbonate chemistry for any given organism might be expected under those conditions where the magnitude and/or frequency of any imposed change exceeds that of current acclimative tolerance (Boyd et al., 2016; Denman, Christian, Steiner, Pörtner & Nojiri, 2011; Joint, Doney & Karl, 2011; Lewis, Brown, Edwards, Cooper & Findlay, 2013; Richier et al., 2014). In addition to dictating the response to experimental manipulation (Richier et al., 2014), differential acclimative potential across organisms may also influence the emergent outcome of community responses to the longer term environmental perturbation represented by OA (Hendricks et al., 2015; Lohbeck, Riebesell & Reusch, 2012; Reusch & Boyd, 2013; Schaum, Rost & Collins, 2016; Schaum, Rost, Millar & Collins, 2013). Indeed, differential sensitivity to dynamic changes in carbonate chemistry might be expected on the basis of theoretical considerations (Flynn et al., 2012) and has recently been demonstrated for phytoplankton, specifically between coastal and open ocean diatom taxa (Li, Wu, Hutchins, Fu & Gao, 2016).

Understanding the fundamental controls on acclimative tolerance to carbonate chemistry variability and adaptive differences in such tolerances between groups and across environmental gradients is essential for predicting natural phytoplankton community responses to OA-type perturbations over space and time (Flynn et al., 2012, 2015; Lewis et al., 2013; Li et al., 2016; Schaum et al., 2016). We, therefore, investigated whether differential responses in the sensitivity of phytoplankton to short-term changes in the CCS were observable within natural communities, and whether such variability related to ocean-scale gradients in environmental conditions. Using a unique data set of 17 mesocosm experiments spanning seven regional seas (i.e., from the Greenland to the Weddell seas) and three ocean regions (from the Arctic to the Southern oceans), we relate observable differential biological responses to the susceptibility of the local system to dynamic changes in carbonate chemistry variables, as quantified by the buffer capacity, while investigating other potentially confounding factors including nutrient availability.

2 | MATERIALS AND METHODS

2.1 | Seawater collection and experimental set up

A series of 17 shipboard multitreatment manipulation experiments were conducted using equivalent protocols on three cruises (Figure 1). The first cruise (D366) took place in northwest European shelf seas during summer on the RRS *Discovery* (2011 June 6–July 12) (Richier et al., 2014). Two subsequent cruises (JR271 and JR274 respectively) were carried out in the Arctic (2012 June 1–July 2) (Poulton et al., 2016) and Southern (2013 January 9–February 12) (Tarling et al., 2016) oceans, both on board the RRS *James Clark Ross*. Locations, oceanographic settings, and treatments applied within each experiment are presented in Tables 1 and 2.

Specific cleaning and handling techniques were followed during setup of each of the experiments. Briefly, the incubation bottles (Polycarbonate, Nalgene™) were acid-cleaned in 1% HCl followed by three de-ionized water (Milli-Q, Millipore) rinses during the low-

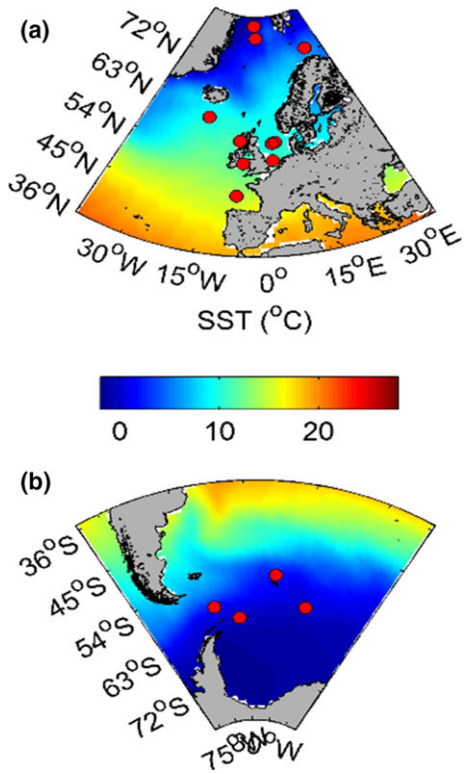

FIGURE 1 Locations of experiments throughout the three cruises. Sea surface temperature (SST; °C) varied markedly across experimental locations (a,b). Red dots illustrate experimental locations

TABLE 1 Bioassay experiment set up conditions. Concentration of nutrients* added to the incubation bottles were the following: +N: 2 μmol/L, +P: 0.2 μmol/L, +Si: 2 μmol/L, +Fe: 2 nmol/L

Cruise	Exp.	Variables manipulated	Conditions	Incubation duration (days)	Sampling points (days)
D366	1	Carbonate chemistry	pCO_2 [550, 750 and 1,000 μatm]	4	0, 2, 4
	2	Carbonate chemistry	pCO_2 [550, 750 and 1,000 μatm]	4	0, 2, 4
	2b	Carbonate chemistry + nutrients	pCO_2 [750 μatm]; nutrients [+N, +P, +NP]*	2	0, 2
	3	Carbonate chemistry	pCO_2 [550, 750 and 1,000 μatm]	4	0, 2, 4
	4	Carbonate chemistry	pCO_2 [550, 750 and 1,000 μatm]	4	0, 2, 4
	4b	Carbonate chemistry + nutrients	pCO_2 [750 μatm]; nutrients [+N, +P, +NP]*	2	0, 2
	5	Carbonate chemistry	pCO_2 [550, 750 and 1,000 μatm]	4	0, 2, 4
	5b	Carbonate chemistry + nutrients	pCO_2 [750 μatm]; nutrients [+N, +P, +NP]*	2	0, 2
JR271	1–5	Carbonate chemistry	pCO_2 [550, 750 and 1,000 μatm]	4	0, 2, 4
JR274	1	Carbonate chemistry + nutrients	pCO_2 [750 μatm];nutrients [+Fe]*	4	0, 2, 4
	2	Carbonate chemistry + nutrients	pCO_2 [750 μatm];nutrients [+Fe]*	6	0, 3, 6
	3	Carbonate chemistry	pCO_2 [750, 1,000 and 2,000 μatm]	6	0, 3, 6
	4	Carbonate chemistry	pCO_2 [750, 1,000 and 2,000 μatm]	8	0, 4, 8

latitude cruise (D366). Further extensive cleaning procedures were applied during cruises in potentially iron-limited regions of the ocean (i.e., high-latitude regions; Figure 1a,b). Bottles, upon first use, were filled up to the neck with detergent (1% Decon) for 1 day followed by three rinses with de-ionized water, and then filled with 10% HCl (Aristar grade) for 3 days followed by three rinses with de-ionized water.

On the day of the experimental setup, vertical profiles of temperature, salinity, oxygen, chlorophyll fluorescence, turbidity, and Photosynthetically Active Radiation (PAR) were obtained in order to select and characterize the depth of experimental water collection within the wider water column (Richier et al., 2014). Unfiltered near-surface (≤33 m) seawater containing the extant natural microbial community was collected at the different stations using Niskin bottles attached to a CTD rosette. The total of up to 480 L of seawater required for each experiment was collected using 24 × 20 L OTE (Ocean Test Equipment) bottles and dispensed from randomly assigned OTE bottles through silicon tubing among 4.5 L (all experiments) or 1.25 L (experiments 2b, 4b, and 5b during D366) polycarbonate bottles.

Multitreatment (≥4 conditions; Table 1) manipulation experiments were incubated in a purposely converted commercial refrigeration container located on the aft deck of the ship. Temperature was maintained (± <1°C) at the in situ value at the time of water collection (Table 2). Irradiance (100 μmol quanta m^{-2} s^{-2}) was provided by daylight simulation LED panels (Powerpax, UK) over a light–dark cycle approximating the ambient photoperiod: 18–6 hr light–dark (D366 and JR274) or 24 hr continuous light (JR271, except for experiment E1 with 18–6 hr).

The majority of experiments (14 of 17) were run for ≥4 days and involved two sampling points following measurement of initial conditions. Independent incubation bottles were sacrificed at every sampling point (Table 1). Specifically, the majority of the experiments (11 of 17) were run using identical durations with sampling points at 0, 2, and 4 days and almost all (14 of 17) included a time point measured after 2 days of incubation, with the shortest resolved timescales often corresponding to the most marked observed biological responses (Richier et al., 2014). The three experiments including inorganic nutrient addition (E2b, E4b, and E5b) during the first cruise (D366) were run under the same temperature and light regime for a shorter incubation period of 2 days with a single sampling point at the end, corresponding to the timescale over which maximum response effects were observed during this cruise (Richier et al., 2014).

Following the failure to observe strong responses within those experiments performed in higher latitude low temperature systems during the second cruise (JR271; Poulton et al., 2016), we subsequently increased incubation timescales for a subset number of experiments on the final cruise (JR274) (Table 1). Specifically, the potential for the observed continued lack of strong responses to be related to slower microbial metabolism within the low temperature waters encountered was investigated by running three experiments of increasingly longer total duration from 4 to 6 to 8 days, and through the inclusion of a higher target pCO_2 condition of 2,000 μatm (Table 1). Subsequently, response magnitudes were found to be independent of overall experimental duration (see below).

2.2 | Variables measured

2.2.1 | Total and size fractionated chlorophyll

Total community chlorophyll concentrations were measured according to the method described in Richier et al. (2014). Briefly, aliquots of 100 mL were sampled from every incubation bottle and filtered onto 25 mm GF/F filters (Whatman, 0.7 μm nominal pore size) or 10-μm pore size polycarbonate filters (Whatman) (to yield a total and a >10 μm size fraction, respectively, and therefore by difference a <10 μm size fraction). Filters were extracted into 6 mL 90% HPLC-

TABLE 2 Initial conditions (average ± *SD*) for the bioassay experiments set up along three cruises. Salinity, depth, and sea surface temperature (SST) were measured in situ using the CTD sensor

Cruise	Exp.	Date	Lat. (°N/S)	Long. (°W/E)	DIC (µmol/kg)	TA (µmol/kg)	pCO_2 (µatm)	SST (°C)	Salinity	Depth (m)	NO_3^- (µmol/L)	PO_4^{3-} (µmol/L)	$Si(OH)_4$ (µmol/L)	Chl *a* (µg/L)
D366	1	8.06.11	56 47.27 N	7 25.01 W	2,091.8 (0.9)	2,310.9 (2.3)	342.74	11.27	34.8	6	1.1 (0.1)	0.1 (0.0)	2.1 (0.2)	3.2 (0.0)
	2	14.06.11	52 28.23 N	5 54.05 W	2,094.5 (0.9)	2,322.2 (2.4)	333.82	11.77	34.44	5	0.3 (0.0)	0.1 (0.0)	0.4 (0.0)	3.5 (0.1)
	2b	19.06.11	46 29.70 N	7 12.67 W	2,085.8	2,345.6	341.05	15.02	35.67	<10	0.9 (0.1)	0.1 (0.0)	1.1 (0.0)	0.5 (0.0)
	3	21.06.11	46 12.14 N	7 13.25 W	2,083.8 (0.6)	2,347.1 (3.6)	340.46	15.31	35.77	10	0.6 (0.0)	0.1 (0.0)	0.6 (0.0)	0.8 (0.0)
	4	26.06.11	52 59.66 N	2 29.84 E	2,085.5 (1.6)	2,295.6 (0.4)	401.90	14.57	34.05	5	0.9 (0.1)	0.1 (0.0)	0.8 (0.0)	1.3 (0.0)
	4b	29.06.11	57 45.93 N	4 35.26 E	2,053.2	2,291.9	327.65	13.09	34.80	<10	0.3	0.0	0.3	0.5 (0.0)
	5	02.07.11	56 30.29 N	3 39.51 E	2,084.6 (1.5)	2,310.8 (3.2)	369.95	13.86	34.99	12	0.3 (0.2)	0.1 (0.0)	0.1 (0.0)	0.2 (0.2)
	5b	03.07.11	59 40.67 N	4 06.92 E	1,997.2	2,214.0	311.35	13.30	30.50	<10	0.3 (0.0)	0.0	0.0	0.8 (0.0)
JR271	1	03.06.12	56 16.00 N	2 37.99 E	2,082.3 (0.5)	2,325.3 (0.4)	300.70	10.78	35.12	10	0.0 (0.0)	0.1 (0.0)	1.3 (0.0)	0.3 (0.0)
	2	08.06.12	60 35.62 N	18 51.39 W	2,086.8 (1.0)	2,323.4 (2.4)	310.29	10.65	35.25	21	5.0 (0.1)	0.3 (0.0)	1.6 (0.2)	1.8 (0.3)
	3	13.06.12	76 10.51 N	2 32.96 W	2,130.0 (3.2)	2,305.3 (6.5)	288.93	1.67	34.93	18	9.2 (0.0)	0.65 (0.0)	5.8 (0.0)	0.9 (0.0)
	4	18.06.12	78 21.15 N	3 39.85 W	2,106.4 (5.7)	2,234.6 (2.9)	303.95	−1.6	32.59	7	4.2 (0.1)	0.79 (0.0)	12.21 (0.0)	3.0 (0.3)
	5	24.06.12	72 53.49 N	26 00.20 E	2,108.7 (2.0)	2,314.0 (4.0)	303.69	6.55	34.97	10	5.38 (0.5)	0.4 (0.0)	3.9 (0.1)	1.2 (0.2)
JR274	1	13.01.13	58 22.00 S	56 15.12 W	2,129.8 (1.1)	2,293.2 (0.8)	305.83	1.94	33.90	33	22.7 (0.1)	1.3 (0.0)	15.5 (0.1)	2.3 (0.1)
	2	18.01.13	61 04.70 S	48 21.58 W	2,145.2 (0.1)	2,281	310.95	−1.44	33.58	19	25.5 (0.2)	1.7 (0.0)	63.5 (0.4)	0.5 (0.1)
	3	25.01.13	52 41.36 S	36 37.28 W	2,152.3 (6.1)	2,287.8	372.15	2.17	33.94	26	24.4 (0.2)	1.6 (0.0)	18.1 (0.1)	0.6 (0.1)
	4	01.02.13	58 05.13 S	25 55.55 W	2,129.5 (4.3)	2,293	286.05	0.51	33.70	19	18.9 (0.6)	1.2 (0.0)	72.4 (0.5)	4.2 (0.4)

grade acetone overnight at 4°C in the dark and fluorescence was then measured using a fluorometer (Turner Designs Trilogy) following Welschmeyer (1994).

2.2.2 | Variable chlorophyll fluorescence (F_v/F_m)

The photosynthetic physiology of total communities was measured according to the method described in Richier et al. (2014) on a Chelsea Scientific Instruments FastTracka II™ Fast Repetition Rate fluorometer (FRRf). Briefly, all samples were dark acclimated for 30 min and FRRf measurements were corrected for the blank effect using carefully prepared 0.2-μm filtrates for all experiments and time points (Cullen & Davis, 2003). F_v/F_m was taken as an estimate of the apparent photosystem II photochemical quantum efficiency (Kolber, Prasil & Falkowski, 1998).

2.2.3 | Particulate organic matter

Measurements of particulate organic carbon, nitrogen, and phosphorous (POC, PON, and POP respectively) were used as indices of relative changes in overall microbial community biomass, noting that detrital material can form a significant component of all of these pools. Although ratios of POC:PON:POP varied across the entire data set (not shown), treatment specific patterns of variability in all these particulate organic matter pools generally covaried (Richier et al., 2014). Consequently, here we only present the most complete data set (POP), noting that conclusions would not differ if using POC or PON, but would be based on a more limited subset of experiments.

Measurements of POP were performed as previously described (Richier et al., 2014). Aliquots of 750 mL of seawater were filtered onto 25-mm glass fibre filters (Fisher MF 300, effective pore size 0.7 μm), which had been precombusted at 400°C, soaked in 10% HCl for 24 hr and rinsed in two subsequent de-ionized water baths for 12 hr each. Following filtration, each filter was oven-dried at 60°C for 8–12 hr and POP content was measured according to the method described in Raimbault, Diaz, Pouvesle and Boudjellal (1999). Briefly, POP compounds were converted into inorganic products by a persulfate wet-oxidation under slightly alkaline conditions. After oxidation, inorganic products were dissolved in a digestion mixture, autoclaved and analysed for phosphate in a Segmented Flow Auto Analyser. In order to estimate the oxidation efficiency of the method, standard organic compounds (Standard reference Material® 1573a) were used.

Overall, up to 39 variables (biological, chemical, and physical) were measured in each of the 17 experiments run during the three cruises (results not shown). Sample treatments and analyses followed the methods described in Richier et al. (2014).

2.3 | Carbonate chemistry manipulation

Sampling was performed on deck for the D366 cruise and inside a trace metal clean container for the two polar cruises (JR271 and JR274).

Subsamples for carbonate chemistry analyses were taken from the CTD at time zero (t_0), and TA and DIC were immediately measured using a TA Titrator (AS-ALK2) and a DIC Analyzer (AS-C3) (Apollo SciTech) respectively. The results were calibrated using measurements of certified reference material obtained from A.G. Dickson (Scripps Institution of Oceanography, USA). The remaining CCS variables were calculated with the CO_2SYS programme (version 1.05) (Lewis & Wallace, 1998; Pierrot, Lewis & Wallace, 2006) run in a MATLAB™ environment and using the carbonic acid dissociation constants of Mehrbach, Culberson, Hawley and Pytkowicz (1973) refitted by Dickson and Millero (1987). The 1σ precisions for DIC and TA measurements were estimated as ±3.8 and ±2.0 μmol/kg respectively (Tynan et al., 2016).

The DIC and TA were subsequently measured on a separate set of manipulated reference bottles at t_0, as well as within all subsequently sampled time point bottles. This checked the performance of the manipulation method, as well as monitored the magnitude of any changes in carbonate chemistry due to ongoing biological activity within the incubation bottles over the experimental duration (Richier et al., 2014; Riebesell & Tortell, 2011). Such changes are presented in Supporting Information Figure S2 with measured pCO_2 typically within 25% of target values at the first time point, while biological activity had generated differences of over 50% from target by the final time points.

Incubation bottles were filled without headspace and immediately manipulated using an equimolar addition of strong acid (1 M HCl) and HCO_3^- (1 M) (Richier et al., 2014). In the case of the polar cruises, trace metal clean HCl (Romil, UHP) was used, and all reagents were precleaned using a Chelex® cation chelation column (Sunda, Price & Morel, 2005). Within a subset of the experiments, inorganic nutrients were also manipulated through addition of major macronutrients (nitrate (NO_3^-), silicic acid (dSi) and phosphate (PO_4^{3-}) or a trace nutrient (DFe) in a factorial manner under both the ambient state of the carbonate system or in addition to being manipulated towards a target pCO_2 (Table 1).

2.4 | Biological replicates and statistical power

Bioassay experiments were set up with seawater collected from either one (D366) or three (JR271 and JR274) dedicated CTDs deployed successively. Independent biological replication, corresponding to a minimum of triplicates per experimental treatment, was maintained subsequent to the initial point of sampling, which corresponded to the closure of a given OTE bottle within the sampled water column, with triplicates during JR271 and JR274 being taken from independent CTD casts. To provide for robust statistical testing of treatment effects alongside sufficient water to perform all required analyses, nine bottles were used for each of the four treatments in three sets of triplicates (see Richier et al. (2014) for further details). Subsamples (n = 3) were collected simultaneously for t_0 measurements of each of the variables to be measured over the subsequent time course (Table 1).

2.5 | Data normalization and statistical analysis

Experimental time courses of biomass and other variable changes were often complex (see below). In order to produce a method of combining data across multiple cruises/environments, individual response variables (e.g., Chl, POP, F_v/F_m) measured across the experimental treatments (i.e., across the range of target pCO_2 levels) were normalized to values measured in control bottles at the same time point. This allows us to derive a normalized effect magnitude for every time point, treatment and variable, that is, for every variable and treatment:

$$\mathrm{Var}_{\mathrm{effect,\ treatment}} = (\mathrm{Var}_{\mathrm{Treatment}} - \mathrm{Var}_{\mathrm{Control}})/\mathrm{Var}_{\mathrm{Control}} \quad (1)$$

For example, the magnitude of the 750 μatm target pCO_2 treatment effect for Chl within an experiment was given by:

$$\mathrm{Chl}_{\mathrm{effect,\ 750}} = (\mathrm{Chl}_{750} - \mathrm{Chl}_{\mathrm{Control}})/\mathrm{Chl}_{\mathrm{Control}} \quad (2)$$

yielding a normalized treatment variable which is equivalent to the net integrated difference in the total community Chl growth rate between the control and the stated (in this case 750 μatm pCO_2) treatment. As a result of differences in sampled time points for some experiments (Table 1) and variability in the magnitude of the treatment effect over time within experiments displaying strong responses (Richier et al., 2014), we also compared maximum differential sensitivities of biological responses to CCS manipulation across the full suite of experiments. Here, we chose the maximum values of the normalized treatment effect over the experimental duration so that the maximal normalized treatment effects (MNTE) represented the maximum observed differential response between a treatment and the control condition over all sampling time points for any given treatment in any given experiment. As discussed elsewhere, the strongest MNTEs were typically observed at the shortest timescales (2 days) resolved (Richier et al., 2014).

Tests for statistical differences ($p < 0.05$) between all treatments and controls were subsequently performed within all individual experiments using one-way ANOVA followed by Tukey–Kramer means comparison tests. For simplicity, here we only quote significant differences between controls and treatments, noting that significant increases in treatment effect as a function of imposed CCS manipulation did occur (Richier et al., 2014). Subsequently, statistically significant correlations ($p < 0.05$, $n = 17$) between the magnitude of treatment effects, as determined by the normalized observed difference between the control treatment and the 750 μatm treatment(s) (i.e., MNTE_{750}) observed across all experiments, and the range of measured initial conditions across all the experiments were assessed using Pearson's product-moment correlation.

3 | RESULTS

3.1 | Variability in responses across environmental settings

Incubation of natural samples alongside manipulations of the carbonate chemistry system (CCS) and nutrients (Table 1) produced complex time-varying responses in many of the performed experiments (Figure 2), likely reflecting the range of different environmental conditions (Table 2) and associated community structures encountered across the full suite of experiments. Overall biomass was observed to increase (e.g., Figure 2a,h,i), remain relatively constant (e.g., Figure 2b,d), or occasionally decline within certain treatments (e.g., Figure 2d,f). Moreover, although addition of the limiting nutrient(s), macronutrients nitrogen (N) and phosphorous (P) for D366 (Richier et al., 2014) and iron (Fe) for JR274 (Figure 2g) invariably resulted in a divergence between treatments, differential treatment effects were only observed as a function of CCS manipulation in a subset of the experiments (e.g., Figure 2d–f). In order to reduce the data and investigate the potential drivers of this observed differential sensitivity to CCS manipulation, we thus calculated MNTEs as described above.

3.2 | Relative responses of microbial communities against latitude

In total, across our full suite of experiments and target pCO_2 levels, up to 48 comparisons between triplicate sets of biological treatments and control bottles were possible, with statistically significant CCS treatment effects expressed as MNTEs observable in around 30% of the comparisons (Figures 3 and 4).

As previously reported (Richier et al., 2014), experiments performed at midlatitudes (Figure 3) consistently revealed relative decreases in net growth, as indicated by total chlorophyll (Chl) accumulation (Figure 3), phytoplankton cell counts (Richier et al., 2014) and indices of overall community biomass (Figure 4), under enhanced pCO_2 (and hence changes in other CCS variables, such as $[H^+]$). In contrast, the apparent photosynthetic efficiency of phytoplankton communities was less affected (Figure 5).

Where statistically significant responses in total community Chl (Figure 3) and microbial biomass accumulation were observed (Figure 4), these effects scaled with the magnitude of the imposed shift in the CCS, with a progressive response such that $\mathrm{MNTE}_{1000} > \mathrm{MNTE}_{750} > \mathrm{MNTE}_{550}$ (Figures 3 and 4). In contrast, no statistically significant responses could typically be detected within identical experiments performed in the Southern Ocean, higher latitude North Atlantic and Arctic Oceans (Figure 3), indicating a prevailing tolerance of polar ocean natural microbial populations to the imposed extreme and rapid changes to the CCS.

3.3 | Drivers for the variable physiological susceptibility across phytoplankton communities

In order to identify potential environmental drivers for the marked variability in the biological responses to CCS manipulation we observed, we considered MNTEs across all 17 experiments and manipulated pCO_2 levels (Figures 3 and 4). In addition to scaling with the magnitude of the imposed experimental manipulation (targeted pCO_2 levels), the observed systematic differences in net total community Chl also scaled with increasing sea surface temperature

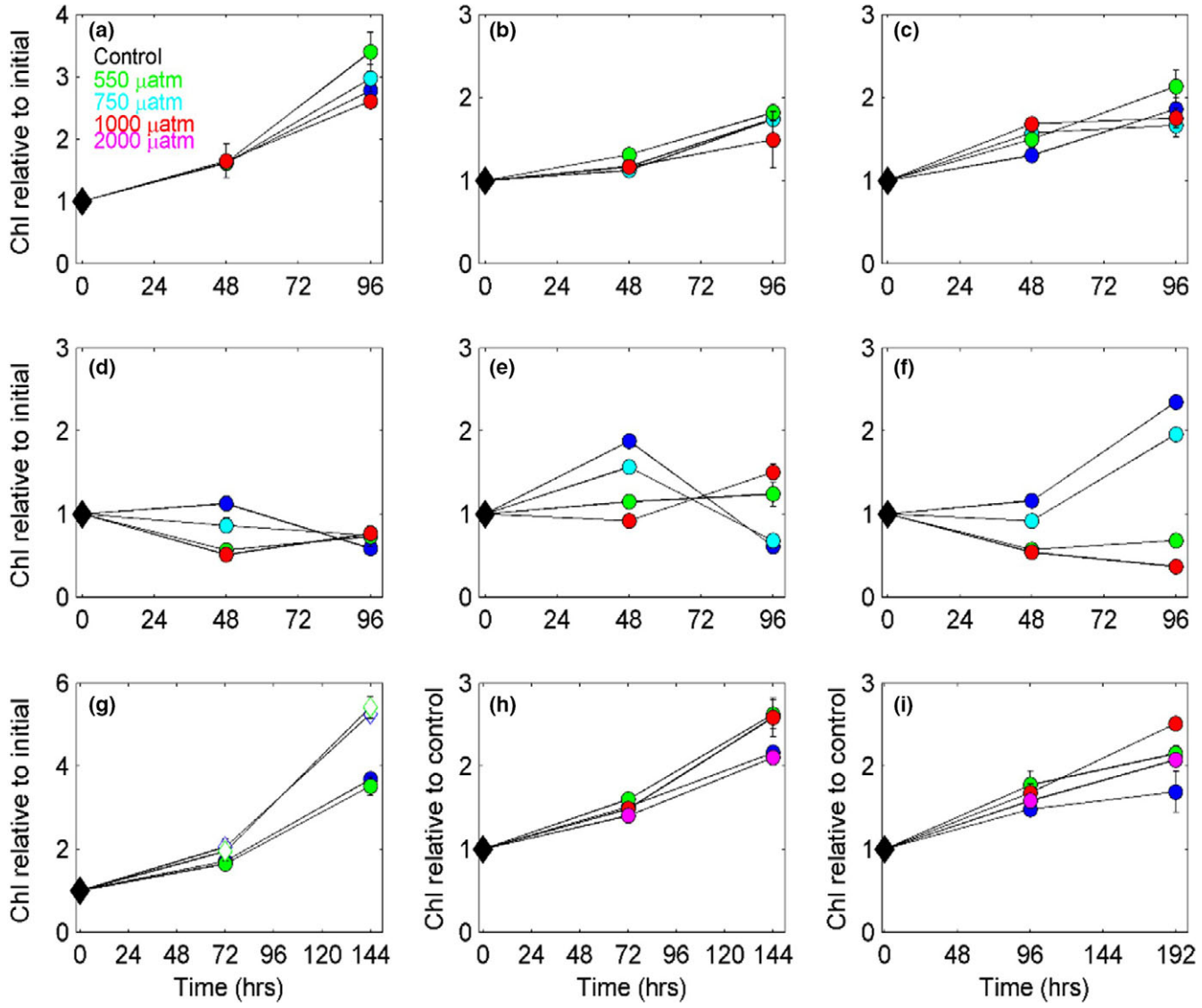

FIGURE 2 Time series measurements of total Chl *a* normalized to initial condition [see Equations 1 and 2] for 9 representative examples from the 17 experiments. Examples plotted are from the Arctic, cruise JR271 experiments 3 (a), 4 (b), and 5 (c), the temperate waters of the European continental shelf, cruise D366 experiments 3 (d), 4 (e), and 5 (f) and the Southern Ocean, cruise JR274, experiments 2 (g), 3 (h), 4 (i). Plotted values are means ±1 *SE*, for biological triplicates, with colours indicating experimental treatment as labelled in (a). Note, open symbols in (g) indicate treatments amended with Fe

(SST) and the correlated increases in buffer capacity (Sundquist, Plummer & Wigley, 1979), as quantified by the H^+ buffer factor ($\beta_{DIC} = (\partial \ \ln[H+]/\partial DIC)^{-1}$) (Figure 4; see Supporting Information) (Egleston et al., 2010).

The increased phytoplankton sensitivity to pCO_2 (and/or $[H^+]$ or other CCS variables) observed under warmer temperatures and higher buffer capacity conditions strongly correlated with, and was dominated by, the response (decreased net growth) of the smaller (<10 µm) size classes (Figure 4 and Supporting Information Figure S1). These coherent responses occurred irrespective of initial nutrient concentrations, which varied considerably between experiments (Table 2). Moreover, while parallel macronutrient and Fe additions (Table 1) enhanced net phytoplankton growth in the European shelf seas and Southern Ocean, respectively, short-term responses to increasing pCO_2 were also observed irrespective of nutrient addition in the latter (Figure 4). The overall MNTE to CCS manipulation within these temperate (>12°C) high buffer capacity waters was of comparable magnitude to the nutrient MNTEs (Figure 6).

Observed responses within our 750 µatm pCO_2 treatments ($MNTE_{750}$) were subsequently compared to a range of initial environmental conditions across all experiments (Figure 7). Decreased net growth rates for bulk community and small sized phytoplankton (<10 µm) were significantly correlated with SST and CCS buffer factors (Figure 7), statistically confirming the patterns observed across the full experimental/treatment data set (Figure 4). Significant correlations were also observed between the bulk phytoplankton responses and both ambient phosphate concentrations and Chl-normalized photosynthetic rates (Figure 7), which also tend to correlate

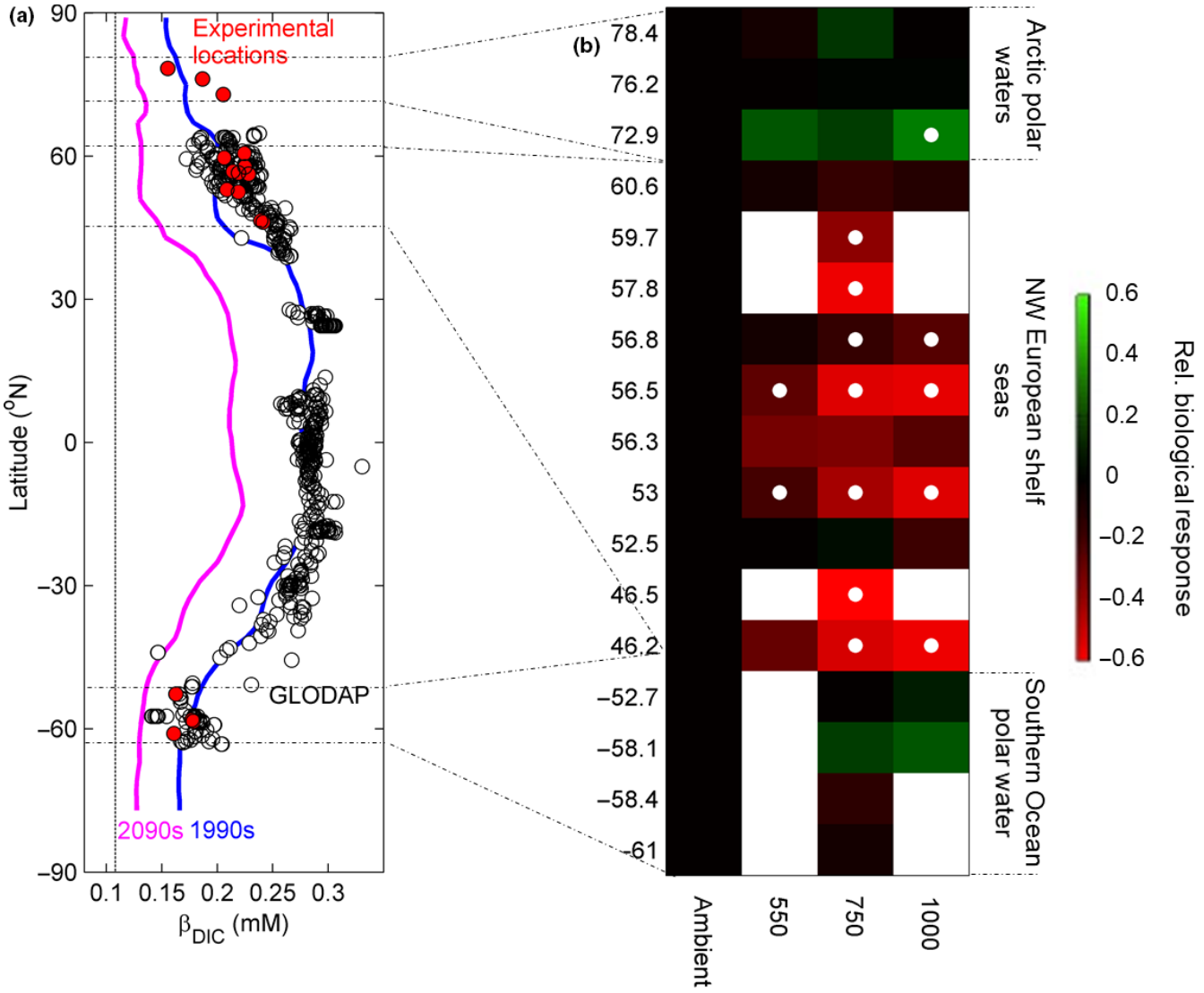

FIGURE 3 Latitudinal gradients in natural buffer factor and relative responses of microbial communities against latitude. Marked natural gradients in the H^+ buffer factor (β_{DIC}) are present in the Atlantic Ocean and were sampled across the full suite of experiments (a). Maximum values of biological responses normalized to controls observed over the duration of each experiment [see Equation 2] presented as a function of treatment and latitude, with the colour scale on the right side indicating the magnitude of response (b). Observed natural large-scale oceanic gradients in in situ buffer factors (a) were derived from the Global Ocean Data Analysis Project (GLODAP) database (Key et al., 2004) with comparative modelled environmental gradients for the 1990s–2090s (dark blue and pink lines respectively) (Yool, Popova, Coward, Bernie & Anderson, 2013). Vertical dotted line in (a) indicates the approximate minimum buffer factors expected as DIC approaches TA (Egleston et al., 2010). Significant differences between treatments and controls in (b) are indicated by white dots (ANOVA, Tukey–Kramer, $p < 0.05$, $N = 3$)

with SST over large oceanic scales (Behrenfeld & Falkowski, 1997; Sundquist et al., 1979). In contrast, differences in net phytoplankton growth rates as a function of imposed treatment displayed no correlation with any of the other wide range of initial physical, chemical, and biological variables tested, including indices of initial community size structure (Figure 7).

4 | DISCUSSION

Combined analysis of a large suite of experiments performed using near-identical protocols on multiple cruises across oceanic scales (Figure 1), revealed differential biological responses which could be related to geographical ambient environmental conditions (Figures 4 and 7). Specifically, the magnitude of observed biological responses to CCS manipulation varied as a function of latitude (Figure 3), in association with correlated variability in ambient nutrient concentration (phosphate), temperature, and CCS buffer capacity (Figure 7). Organism responses to environmental forcing may vary as a function of interactions between any one or more such environmental drivers (Boyd et al., 2010, 2016). For example, responses to CCS manipulation may vary as a function of nutrient availability (Li, Gao & Beardall, 2012; Richier et al., 2014; Trimborn et al., 2017), while temperature will also directly influence metabolic rates and

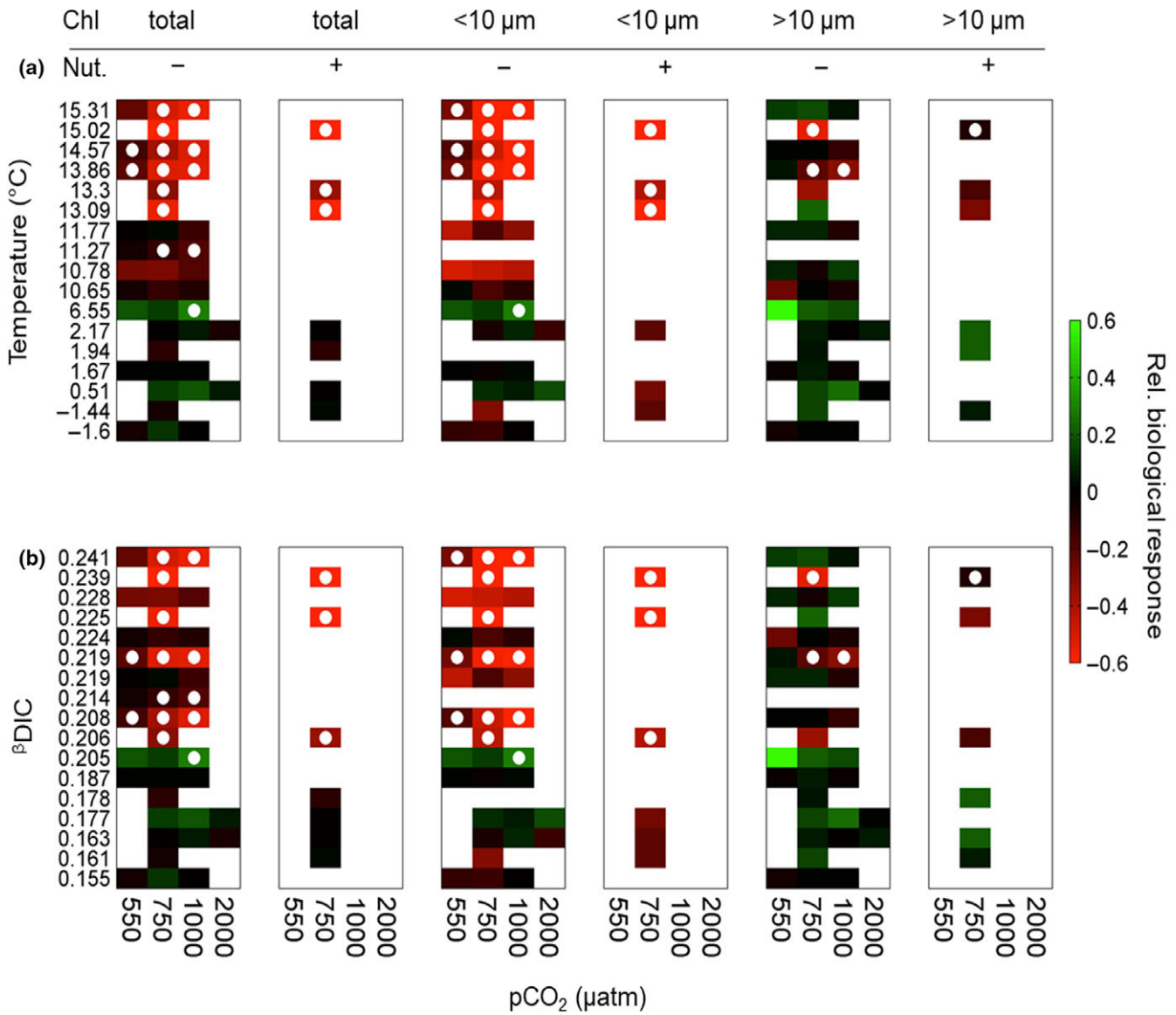

FIGURE 4 Ranked relative biological responses of natural microbial communities to altered pCO_2. Observed maximum values of control normalized experimental responses to increased pCO_2 across all 17 natural microbial communities analysed. Phytoplankton responses are presented for total and size fractionated (<10 μm or >10 μm) Chl across all measured target pCO_2 concentrations under experimental conditions with ('−') or without ('+') additional nutrient (Nut.) amendment. Experimental results were ranked in order of (a) ambient sea surface temperature (SST, °C) or (b) initial H^+ buffer factor (β_{DIC}). Calculations, colour scales, and statistical tests are as described for Figure 3b

potentially interact with variability in the CCS to determine organism responses (Flynn et al., 2012; Humphreys, 2017).

In terms of nutrient availability, although MNTEs correlated with phosphate availability (Figure 7), this was unlikely to be causative. Similar responses could be observed within both our ambient and nutrient replete experimental treatments (Figures 4 and 6), with overall treatment effects being of a similar magnitude within the higher temperature lower buffer capacity waters irrespective of nutrient condition (Figure 6). Although we cannot fully discount a potential direct influence of temperature on the observed differential responses (Figure 7), we argue that any such influence would have to be through an unknown (eco-)physiological mechanism rather than simply being an artefact of experimental duration. Specifically, maximum net growth rates might be expected to be around two- to threefold higher in the warmest compared to the coldest waters sampled (Eppley, 1972). Consistent with such expectation, maximum Chl-normalized photosynthetic rates were around two- to threefold higher (Figure 7) in the lower latitude experiments, as were net growth rates within our nutrient replete experimental treatments (0.19–0.27 day^{-1} for SST < 3°C vs. 0.28–0.68 day^{-1} for SST > 12°C). However, CCS responses in the high-latitude experiments remained insignificant, despite a subset of these being up to twice the overall experimental duration (Figure 2h,i; Table 1) and four times longer than the 2 day time point where MNTEs were typically observed within the midlatitude experiments (Figure 2).

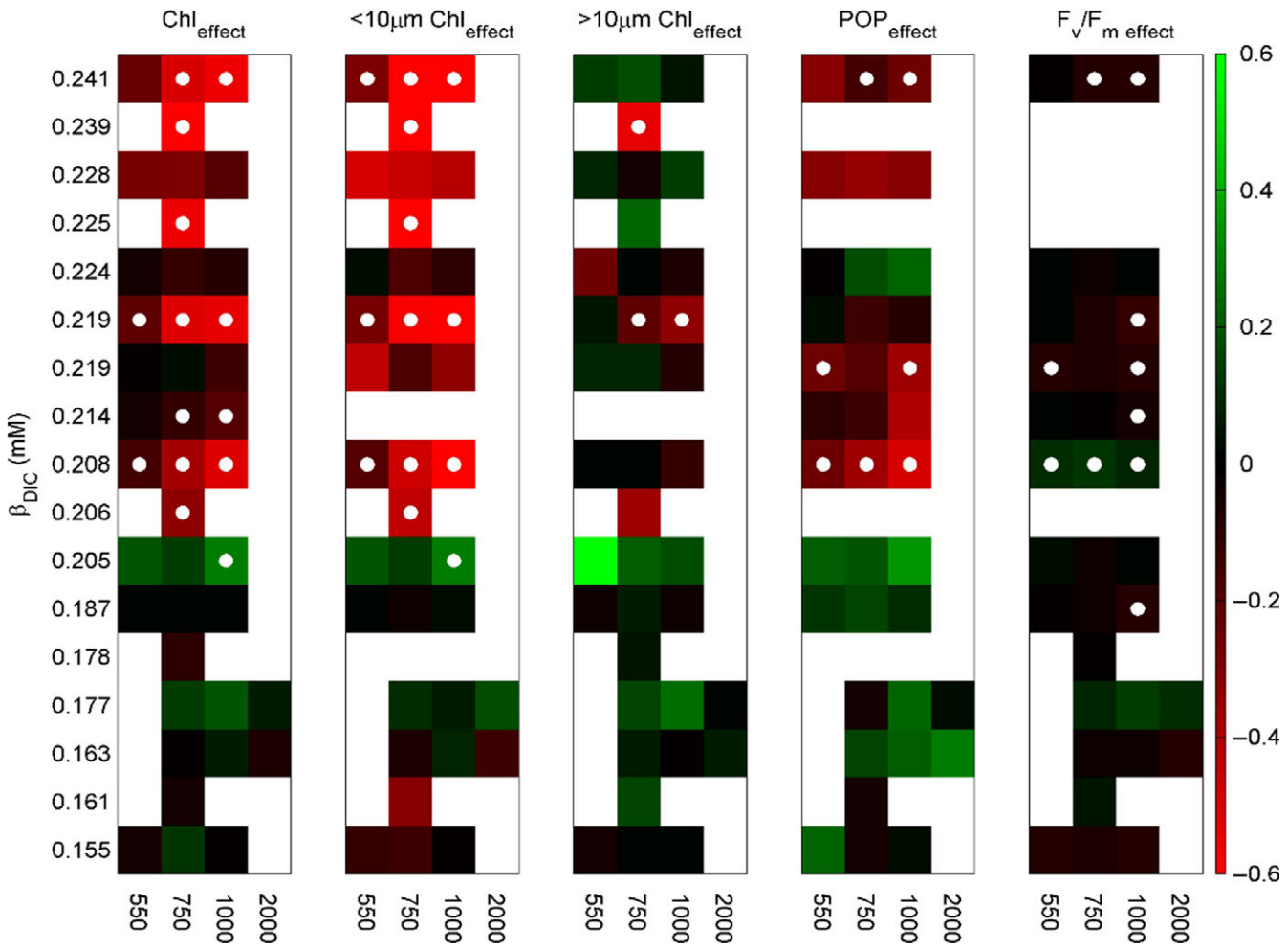

FIGURE 5 Response magnitudes of different variables ordered as a function of initial H^+ buffer factor (β_{DIC}). Colour scale on the right side indicates the magnitude of response with abbreviations, calculations and significant differences between treatments all as described for Figures 3 and 4

Although we cannot unequivocally relate causation to correlation, we argue that the association of the strongest MNTEs with the lowest buffer capacity waters (Figure 7) is consistent with theoretical expectations and previous arguments (Flynn et al., 2012; Richier et al., 2014). Specifically, the magnitude of natural CCS variability encountered by an aquatic organism is a complex function of external forcing (Hofmann et al., 2011), buffering capacity (Glas, Fabricius, de Beer & Uthicke, 2012; Hofmann, Middelburg, Soetaert, Wolf-Gladrow & Meysman, 2010), behaviour (Lewis et al., 2013), cell morphology (Flynn et al., 2012; Hurd et al., 2011), metabolic rate (Chrachri, Hopkinson, Flynn, Brownlee & Wheeler, 2018; Flynn et al., 2012), and diffusional transport constraints (Glas et al., 2012). All of these factors may interact (Flynn et al., 2012; Glas et al., 2012; Hofmann et al., 2011; Richier et al., 2014) across a broad range of temporal (from hours to days; Hofmann et al., 2011) and spatial (from single organism to ecosystem; Hendricks et al., 2015) scales.

At cellular scales, the microenvironment at the vicinity of the cell, or diffusive boundary layer (DBL), decouples chemical concentrations at the cell surface from those within the surrounding seawater (Chrachri et al., 2018; Wolf-Gladrow, Bijma & Zeebe, 1999; Zeebe, Wolf-Gladrow, Bijma & Hornisch, 2003), potentially mediating physiological susceptibility to CCS variability (Flynn et al., 2012; Glas et al., 2012; Hurd et al., 2011). Indeed, feedbacks between metabolic processes (photosynthesis, respiration, calcification) and subsequent CCS variability at the cell surface is highly dependent on the thickness of the DBL (Flynn et al., 2012). Moreover, the thickness of the DBL is itself a function of both cell morphology/cell size (Finkel et al., 2010; Flynn et al., 2012) and ambient seawater flow regime (Glas et al., 2012; Hurd et al., 2011). Consequently, large-celled phytoplankton with thicker DBLs would be expected to experience higher natural CCS variability at the cell surface and hence have a higher inherent tolerance to external CCS forcing than smaller cells (Flynn et al., 2012; Richier et al., 2014).

The observed differential sensitivity of phytoplankton communities to imposed CCS variability within our combined data set (Figures 3, 4 and 7) is thus consistent with such theoretical considerations (Flynn et al., 2012). Specifically, enhanced susceptibility to rapid CCS changes for natural communities sampled under high buffer capacity conditions may reflect a lower tolerance to external changes in CCS under conditions where natural variability

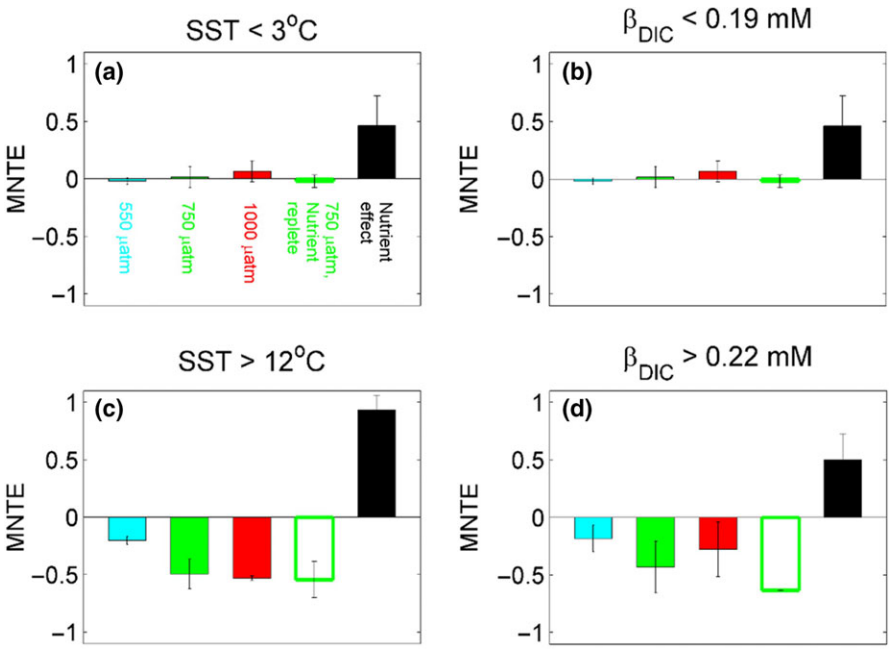

FIGURE 6 Maximal normalized treatment effects (MNTE) to variations in chemical species and nutrient addition. Maximal effects in response to pCO_2 (and hence $[H^+]$ etc.) manipulation and nutrient addition across all experiments grouped as (a,c) a function of temperature (°C) and (b, d) initial H^+ buffer capacity (β_{DIC}). Plotted values are means ±1 *SE* of the mean normalized responses across all experiments

both within bulk seawater and the DBL is lower (Flynn et al., 2012). It is therefore logical to expect that this mechanism would be amplified for smaller cells with thinner DBLs, where the influence of bulk seawater buffering capacity on cell surface buffering should be greatest (Flynn et al., 2012; Richier et al., 2014) (Figures 4 and 7).

Given the short timescale of the anthropogenic perturbation compared to phytoplankton generation and hence evolutionary timescales (Lohbeck et al., 2012; Schaum et al., 2013, 2016), let alone that of short-term experimental manipulations (Joint et al., 2011), the implications of the proposed mechanisms in the context of future OA remain difficult to specify. The most marked responses that we observed typically occurred over the shortest timescales resolved (2 days) (Richier et al., 2014), with less pronounced differences observable over timescales ≥72 hr (Figure 2) when, in some cases, in the absence of additional nutrient enrichment, nutrient exhaustion may have driven the system to a similar state across all treatments (Richier et al., 2014). However, we suggest that the observed dominance of short response timescales could also reflect subsequent rapid acclimation of the measured phytoplankton populations following an initial stress response caused by the experimental manipulation forcing the small cell sized subpopulation outside of their extant acclimative tolerance range.

In addition to our observed short timescale responses not being simply scalable to longer timescales, our results also do not preclude the potential importance of other drivers of interactions between phytoplankton and the CCS, either within experimental studies or under altered future conditions (Riebesell & Tortell, 2011). For example, elevated pCO_2 may also directly facilitate enhanced growth rates, in particular for larger celled phytoplankton (Riebesell & Tortell, 2011; Wu et al., 2014). Minor positive treatment effects in our lower latitude experiments (Figure 3) would be consistent with such a mechanism, although these observations were not typically significant.

Our results suggest that both short- and long-term experiments (Tatters, Roleda et al., 2013; Tatters, Schnetzer et al., 2013) investigating the impact of OA may need careful interpretation, as any extant organism lacking in acclimative tolerance to rapid CCS changes might be disadvantaged and hence selected against in the early stages of any CCS manipulation experiment. Although initial community size structure was not a significant predictor of the differential responses (Figure 7) (Richier et al., 2014), both community composition and the history of prior environmental fluctuations, as mediated by buffer capacity, may thus influence the outcome of experiments over a range of timescales. More broadly, these also influence the selective and evolutionary outcomes of interactions between phytoplankton communities and CCS forcing (Flynn et al., 2015; Li et al., 2016; Schaum et al., 2016).

Oceanic uptake of anthropogenic CO_2 will continue to decrease the CCS buffer capacity in the future (Egleston et al., 2010; Schaum et al., 2016). Spatial gradients in buffer capacity will also decrease as buffering approaches a minimum where dissolved inorganic carbon (DIC) and total alkalinity (TA) converge (Figure 2a) (Egleston et al., 2010). Although our experiments covered a significant range of extant buffer capacity variability in the oceans (Figure 3a), extension to lower latitude, higher buffer capacity systems would be desirable in future studies. Indeed, low-latitude oligotrophic waters with high buffering capacity will experience the greatest absolute changes in the future (Figure 3a), with up to 22% decreases in resistance to $[H^+]$ variation (Egleston et al., 2010) and corresponding increases in the degree of CCS variability.

In contrast, cold DIC-rich high-latitude systems such as that we sampled in the Southern Ocean, high-latitude North Atlantic and Arctic will be subject to lower decreases, with buffer factors potentially approaching theoretical minima around the end of this century (Figure 3a) (Orr et al., 2005). Relative changes in the degree of near

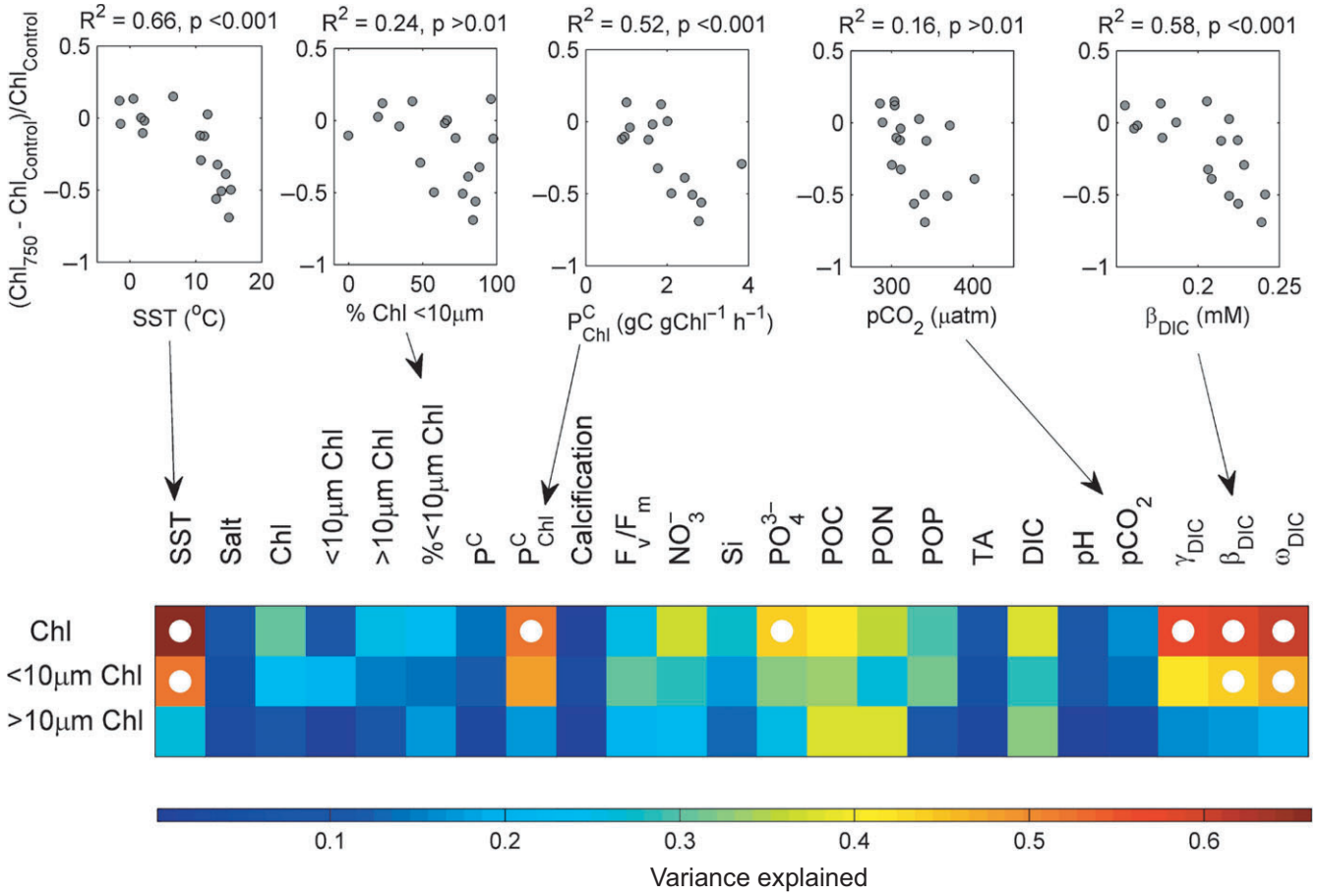

FIGURE 7 Correlation between indices of normalized phytoplankton responses under the 750 μatm pCO_2 treatment and representative initial conditions. Scatter plots of whole community (total Chl) normalized phytoplankton responses in the 750 μatm treatment are presented against representative initial conditions (top), alongside a heat map of correlation coefficients between three indices of phytoplankton responses in the 750 μatm treatment and the complete set of available initial conditions. The following abbreviations are used: sea surface temperature (SST); Chlorophyll (Chl); photosynthetic rate (P^C); Chl-normalized photosynthetic rate (P^C_{Chl}); apparent photochemical quantum efficiency (F_v/F_m); particulate organic carbon (POC); particulate organic nitrogen (PON); particulate organic phosphorous (POP); total alkalinity (TA); dissolved inorganic carbon (DIC); [CO_2], [H^+] and carbonate saturation state (Ω) buffer factors (γ_{DIC}, β_{DIC}, and ω_{DIC}, respectively, see Supporting Information for details on buffer factors calculation). Correlation analyses between initial conditions and the presented responses [total and size fractionated (<10 μm and >10 μm Chl)] were performed across all 17 experiments with data normalized to the control treatment as described in Figure 3b. White dots indicate significant correlations between responses and initial conditions ($p < 0.01$)

cell surface CCS variability (Chrachri et al., 2018; Egleston et al., 2010; Flynn et al., 2012) will be larger in midlatitude temperate systems, but largest in the potentially expanding (Polovina, Howell & Abecassis, 2008; Sarmiento et al., 2004) low-latitude oligotrophic systems. These environments, where extant phytoplankton communities are typically dominated by small celled taxa (Finkel et al., 2010), might be expected to display the lowest inherent acclimative tolerance to CCS variability. Increased [H^+] variability may therefore have the greatest potential to drive adaptive responses of microbial communities (Flynn et al., 2012; Lewis et al., 2013), through a combination of selection or evolution (Schaum et al., 2016), in such low-latitude systems.

Geographically related sensitivities of upper ocean phytoplankton communities to imposed rapid changes in the CCS (Figure 2) cautions against simple extrapolation of single or geographically limited experimental results (Joint et al., 2011). Regional environmental variability, including the potential role of decreased seawater buffer capacity and any associated ecosystem feedbacks, needs to be considered alongside a taxonomic, functional group and evolutionary perspective (Collins et al., 2014; Flynn et al., 2015; Schaum et al., 2013, 2016).

The overall consequences of any buffer capacity and cell size-related acclimative tolerances to CCS variability (Figures 3, 4 and 7) for marine ecosystems and subsequent perturbations to biogeochemical cycles will likely depend on the magnitude of the metabolic costs associated with adaptation to a more variable environment. It is plausible that CCS fluctuations at the cell surface, as a function of cell size (Flynn et al., 2012), location (Hofmann et al., 2011), and altered forcing (Egleston et al., 2010), may influence selection (Gaitán-Espitia et al., 2017; Li et al., 2016; Schaum et al., 2016) and contribute to shifts in phytoplankton community structure (Finkel et al., 2010). For example, energetic costs incurred by organisms

requiring higher active H^+ and/or HCO_3^- transport for cellular homeostasis purposes (Flynn et al., 2012; Taylor, Brownlee & Wheeler, 2012), may trade-off against the consequences of poorer cellular acid-base regulation or the requirement to be smaller (Schlüter et al., 2014). Despite any remaining ecophysiological uncertainties, our study highlights how organism and ecosystem responses to OA need to be considered not only in the context of changes to the mean CCS state but also in relation to the magnitude of CCS variability experienced by organisms at cellular scales (Chrachri et al., 2018; Flynn et al., 2012; Schaum et al., 2016). We suggest that these factors may be fundamentally linked to the regionally variable buffering characteristics of oceanic waters.

ACKNOWLEDGEMENTS

This work was funded under the UK Ocean Acidification (UKOA) programme via Natural Environment Research Council grants NE/H017348/1 to T. Tyrrell, E. P. Achterberg, and C. M. Moore; NE/H017097/1 to A. J. Poulton; NE/H017062/1 to D. J. Suggett and a studentship to M. P. Humphreys. Contributions to D. J. Suggett were also supported through an Australian Research Council Future Fellowship (FT130100202). We thank C. Dumousseaud, M. Ribas-Ribas, and E. Tynan for processing carbonate chemistry analyses and M. Stinchcombe for nutrient data. We are also grateful to A. Yool for the model output and to T. Bibby and D. Allemand for discussions and/or comments on the manuscript.

AUTHOR CONTRIBUTION

C.M.M., E.P.A., A.J.P., T.T., and D.J.S. designed the research. C.M.M., S.R., A.J.P., T.T., and D.J.S. conceived and designed the experiments. S.R., C.M.M., E.P.A., A.J.P., T.T., and D.J.S. performed the experiments. S.R. and C.M.M. analysed and interpreted the data. S.R. and C.M.M. wrote the manuscript. All authors contributed to discussions of the results and subsequent editing of the paper.

ORCID

Sophie Richier http://orcid.org/0000-0001-5485-3525
Matthew P. Humphreys http://orcid.org/0000-0002-9371-7128
Alex J. Poulton http://orcid.org/0000-0002-5149-6961
David J. Suggett http://orcid.org/0000-0001-5326-2520

REFERENCES

Bach, L. T., Riebesell, U., Gutowska, M. A., Federwisch, L., & Schulz, K. G. (2015). A unifying concept of coccolithophore sensitivity to changing carbonate chemistry embedded in an ecological framework. *Progress in Oceanography*, *135*, 125–138. https://doi.org/10.1016/j.pocean.2015.04.012

Behrenfeld, M. J., & Falkowski, P. G. (1997). Photosynthetic rates derived from satellite-based chlorophyll concentration. *Limnology and Oceanography*, *42*, 1–20. https://doi.org/10.4319/lo.1997.42.1.0001

Boyd, P. W. (2011). Beyond ocean acidification. *Nature Geoscience*, *4*, 273–274. https://doi.org/10.1038/ngeo1150

Boyd, P. W., Cornwall, C. E., Davison, A., Doney, S. C., Fourquez, M., Hurd, C. L., … McMinn, A. (2016). Biological response to environmental heterogeneity under future ocean conditions. *Global Change Biology*, *22*, 2633–2650. https://doi.org/10.1111/gcb.13287

Boyd, P. W., Lennartz, S. T., Glover, D. M., & Doney, S. C. (2015). Biological ramifications of climate-change mediated oceanic multi-stressors. *Nature Climate Change*, *5*, 71–79. https://doi.org/10.1038/nclimate2441

Boyd, P. W., Strzepek, R., Fu, F. X., & Hutchins, D. A. (2010). Environmental control of open-ocean phytoplankton groups: Now and in the future. *Limnology and Oceanography*, *55*, 1353–1376. https://doi.org/10.4319/lo.2010.55.3.1353

Chrachri, A., Hopkinson, B. M., Flynn, K., Brownlee, C., & Wheeler, G. L. (2018). Dynamic changes in carbonate chemistry in the microenvironment around single marine phytoplankton cells. *Nature Communications*, https://doi.org/10.1038/s41467-017-02426-y

Collins, S., Rost, R., & Rynearson, T. A. (2014). Evolutionary potential of marine phytoplankton under ocean acidification. *Evolutionary Applications*, *7*, 140–155. https://doi.org/10.1111/eva.12120

Cullen, J., & Davis, R. (2003). The blank can make a big difference in oceanographic measurements. *Limnology and Oceanography Bulletin*, *12*, 29–35. https://doi.org/10.1002/lob.200312229

Denman, K., Christian, J. R., Steiner, N., Pörtner, H.-O., & Nojiri, Y. (2011). Potential impacts of future ocean acidification on marine ecosystems and fisheries: Current knowledge and recommendations for future research. *ICES Journal of Marine Science*, *68*, 1019–1029. https://doi.org/10.1093/icesjms/fsr074

Dickson, A. G., & Millero, F. J. (1987). A comparison of the equilibrium constants for the dissociation of carbonic acid in seawater media. *Deep Sea Research Part II*, *34*, 1733–1743. https://doi.org/10.1016/0198-0149(87)90021-5

Doney, S. C., Fabry, V. J., Feely, R. A., & Kleypas, J. A. (2009). Ocean acidification: The other CO_2 problem. *Annual Review of Marine Science*, *1*, 169–192. https://doi.org/10.1146/annurev.marine.010908.163834

Dutkeiwicz, S., Morris, J. J., Follows, M. J., Scott, J., Levitan, O., Dyhrman, S. T., & Berman-Frank, I. (2015). Impact of ocean acidification on the structure of future phytoplankton communities. *Nature Climate Change*, *5*, 1002–1006. https://doi.org/10.1038/nclimate2722

Egleston, E. S., Sabine, C. L., & Morel, F. M. M. (2010). Revelle revisited: Buffer factors that quantify the response of ocean chemistry to changes in DIC and alkalinity. *Global Biogeochemical Cycles*, *24*, GB1002.

Eppley, R. W. (1972). Temperature and phytoplankton growth in the sea. *Fishery Bulletin*, *70*, 1063–1085.

Finkel, Z. V., Beardall, J., Flynn, K. J., Quigg, A., Rees, T. A. V., & Raven, J. A. (2010). Phytoplankton in a changing world: Cell size and elemental stoichiometry. *Journal of Plankton Research*, *32*, 119–137. https://doi.org/10.1093/plankt/fbp098

Flynn, K. J., Blackford, J. C., Baird, M. E., Raven, J. A., Clark, D. R., Beardall, J., … Wheeler, G. L. (2012). Changes in pH at the exterior surface of plankton with ocean acidification. *Nature Climate Change*, *2*, 510–513.

Flynn, K. J., Clark, D. R., Mitra, A., Fabian, H., Hansen, P. J., Glibert, P. M., … Brownlee, C. (2015). Ocean acidification with (de)eutrophication will alter future phytoplankton growth and succession. *Proceedings of the Royal Society of London B*, *282*, 20142604. https://doi.org/10.1098/rspb.2014.2604

Frankignoulle, M. A. (1994). Complete set of buffer factors for acid/base CO_2 system in seawater. *Journal of Marine Systems*, *5*, 111–118. https://doi.org/10.1016/0924-7963(94)90026-4

Gaitán-Espitia, J. D., Marshall, D., Dupont, S., Bacigalupe, L. D., Bodrossy, L., & Hobday, A. J. (2017). Geographical gradients in selection can

reveal genetic constraints for evolutionary responses to ocean acidification. *Biology Letters*, *13*, 20160784. https://doi.org/10.1098/rsbl.2016.0784

Glas, M. S., Fabricius, K. E., de Beer, D., & Uthicke, S. (2012). The O_2, pH and Ca^{2+} microenvironment of benthic foraminifera in a high CO_2 world. *PLoS ONE*, *7*, e50010. https://doi.org/10.1371/journal.pone.0050010

Hendricks, I. E., Duarte, C. M., Olsen, Y. S., Steckbauer, A., Ramajo, L., Moore, T. S., … McCulloch, M. (2015). Biological mechanisms supporting adaptation to ocean acidification in coastal ecosystems. *Estuarine, Coastal and Shelf Science*, *152*, A1–A8. https://doi.org/10.1016/j.ecss.2014.07.019

Hofmann, A. F., Middelburg, J. J., Soetaert, K., Wolf-Gladrow, D. A., & Meysman, F. J. R. (2010). Proton cycling, buffering, and reaction stoichiometry in natural waters. *Marine Chemistry*, *121*, 246–255. https://doi.org/10.1016/j.marchem.2010.05.004

Hofmann, G. E., Smith, J. E., Johnson, K. S., Send, U., Levin, L. A., Micheli, F., … Martz, T. R. (2011). High-frequency dynamics of ocean pH: A multi-ecosystem comparison. *PLoS ONE*, *6*, e28983. https://doi.org/10.1371/journal.pone.0028983

Hoppe, C. J., Hassler, C. S., Payne, C. D., Tortell, P. D., Rost, B., & Trimborn, S. (2013). Iron limitation modulates ocean acidification effects on southern ocean phytoplankton communities. *PLoS ONE*, *8*, e79890. https://doi.org/10.1371/journal.pone.0079890

Humphreys, M. P. (2017). Climate sensitivity and the rate of ocean acidification: Future impacts, and implications for experimental design. *ICES Journal of Marine Science*, *74*, 934–940.

Hurd, C. L., Cornwall, C. E., Currie, K., Hepburn, C. D., McGraw, C. M., Hunter, K. A., & Boyd, P. W. (2011). Metabolically induced pH fluctuations by some coastal calcifiers exceed projected 22nd century ocean acidification: A mechanism for differential susceptibility? *Global Change Biology*, *17*, 3254–3262. https://doi.org/10.1111/j.1365-2486.2011.02473.x

Joint, I., Doney, S. C., & Karl, D. M. (2011). Will ocean acidification affect marine microbes? *ISME Journal*, *5*, 1–7. https://doi.org/10.1038/ismej.2010.79

Key, R. M., Kozyr, A., Sabine, C. L., Lee, K., Wanninkhof, R., Bullister, J. L., … Peng, T.-H. (2004). A global ocean carbon climatology: Results from global data analysis project (GLODAP). *Global Biogeochemical Cycle*, *18*, GB4031.

Kolber, Z. S., Prasil, O., & Falkowski, P. G. (1998). Measurements of variable chlorophyll fluorescence using fast repetition rate techniques: Defining methodology and experimental protocols. *BBA – Bioenergetics*, *1367*, 88–106. https://doi.org/10.1016/S0005-2728(98)00135-2

Kroeker, K. J., Kordas, R. L., Crim, R., Hendriks, I. E., Ramajo, L., Singh, G. S., … Gattuso, J.-P. (2013). Impacts of ocean acidification on marine organisms: Quantifying sensitivities and interaction with warming. *Global Change Biology*, *19*, 1884–1896. https://doi.org/10.1111/gcb.12179

Lewis, C. N., Brown, K. A., Edwards, L. A., Cooper, G., & Findlay, H. S. (2013). Sensitivity to ocean acidification parallels natural pCO_2 gradients experienced by Arctic copepods under winter sea ice. *Proceedings of the National Academy of Sciences USA*, *110*, E4960–E4967. https://doi.org/10.1073/pnas.1315162110

Lewis, E., & Wallace, D. W. R. (1998). *Program developed for CO_2 system calculations*. ORNL/CDIAC-105. Oak Ridge, TN: Carbon Dioxide Information Analysis Center, Oak Ridge National Laboratory, US Department of Energy. https://doi.org/10.2172/639712

Li, W., Gao, K., & Beardall, J. (2012). Interactive effects of OA and N-limitation on the diatom *Phaeodactylum tricornutum*. *PLoS ONE*, *7*, e51590. https://doi.org/10.1371/journal.pone.0051590

Li, F., Wu, Y., Hutchins, D. A., Fu, F., & Gao, K. (2016). Physiological responses of coastal and oceanic diatoms to diurnal fluctuations in seawater carbonate chemistry under two CO_2 concentrations. *Biogeosciences*, *13*, 6247–6259. https://doi.org/10.5194/bg-13-6247-2016

Lohbeck, K. T., Riebesell, U., & Reusch, T. H. (2012). Adaptive evolution of a key phytoplankton species to ocean acidification. *Nature Geoscience*, *5*, 346–351. https://doi.org/10.1038/ngeo1441

Mehrbach, C., Culberson, C. H., Hawley, J. E., & Pytkowicz, R. M. (1973). Measurement of apparent dissociation-constants of carbonic-acid in seawater at atmospheric pressure. *Limnology and Oceanography*, *18*, 897–907. https://doi.org/10.4319/lo.1973.18.6.0897

Muller, M. N., Trull, T. W., & Hallegraeff, G. M. (2017). Independence of nutrient limitation and carbon dioxide impacts on the Southern Ocean coccolithophore *Emiliania huxleyi*. *The ISME Journal*, *11*, 1777–1787. https://doi.org/10.1038/ismej.2017.53

Orr, J. C., Fabry, V. J., Aumont, O., Bopp, L., Doney, S. C., Feely, R. A., … Yool, A. (2005). Anthropogenic ocean acidification over the twenty-first century and its impact on calcifying organisms. *Nature*, *437*, 681–686. https://doi.org/10.1038/nature04095

Pierrot, D., Lewis, E., & Wallace, D. W. R. (2006). *MS Excel program developed for CO_2 system calculations*, *ORNL/CDIAC-105*. Oak Ridge, TN: Carbon Dioxide Information Analysis Center, Oak Ridge National Laboratory, US Department of Energy.

Polovina, J. J., Howell, E. A., & Abecassis, M. (2008). Ocean's least productive waters are expanding. *Geophysical Research Letters*, *35*, L03618.

Poulton, A. J., Daniels, C. J., Esposito, M., Humphreys, M. P., Mitchell, E., Ribas-Ribas, M., … Richier, S. (2016). Production of dissolved organic carbon by Arctic plankton communities: Responses to elevated carbon dioxide and the availability of light and nutrients. *Deep Sea Research Part II*, *127*, 60–74. https://doi.org/10.1016/j.dsr2.2016.01.002

Raimbault, P., Diaz, F., Pouvesle, W., & Boudjellal, B. (1999). Simultaneous determination of particulate organic carbon, nitrogen and phosphorus collected on filters, using a semi-automatic wet-oxidation method. *Marine Ecology Progress Series*, *180*, 289–295. https://doi.org/10.3354/meps180289

Reusch, T. B. H., & Boyd, P. W. (2013). Experimental evolution meets marine phytoplankton. *Evolution*, *67*, 1849–1859. https://doi.org/10.1111/evo.12035

Richier, S., Achterberg, E. P., Dumousseaud, C., Poulton, A. J., Suggett, D. J., Tyrrell, T., … Moore, C. M. (2014). Phytoplankton responses and associated carbon cycling during shipboard carbonate chemistry manipulation experiments conducted around Northwest European shelf seas. *Biogeosciences*, *11*, 4733–4752. https://doi.org/10.5194/bg-11-4733-2014

Riebesell, U., Bach, L. T., Bellerby, R. G. J., Bermudez Monsalve, J. R., Boxhammer, T., Czerny, J., … Schulz, K. G. (2017). Competitive fitness of a predominant pelagic calcifier impaired by ocean acidification. *Nature Geoscience*, *10*, 19–23. https://doi.org/10.1038/ngeo2854

Riebesell, U., & Tortell, P. D. (2011). Effects of ocean acidification on pelagic organisms and ecosystems. In J.-P. Gattuso & L. Hansson (Eds.), *Ocean acidification* (pp. 99–121). Oxford, UK: University of Oxford Press.

Royal Society (2005). *Ocean acidification due to increasing atmospheric carbon dioxide*, *60*, *Policy Document 12/05*. London, UK: The Royal Society.

Sarmiento, J. L., Slater, R., Barber, R., Bopp, L., Doney, S. C., Hirst, A. C., … Soldatov, V. (2004). Response of ocean ecosystems to climate warming. *Global Biogeochemical Cycle*, *18*, GB3003.

Schaum, C. E., Rost, B., & Collins, S. (2016). Environmental stability affects phenotypic evolution in a globally distributed marine picoplankton. *ISME Journal*, *10*, 75–84. https://doi.org/10.1038/ismej.2015.102

Schaum, C. E., Rost, B., Millar, A. J., & Collins, S. (2013). Variation in plastic responses of a globally distributed picoplankton species to ocean acidification. *Nature Climate Change*, *3*, 298–302. https://doi.org/10.1038/nclimate1774

Schlüter, L., Lohbeck, K. T., Gutowska, M. A., Gröger, J. P., Riebesell, U., & Reusch, T. B. H. (2014). Adaptation of a globally important coccolithophore to ocean warming. *Nature Climate Change*, *4*, 1024–1030. https://doi.org/10.1038/nclimate2379

Sunda, W. G., Price, N. M., & Morel, F. M. M. (2005). Trace metal ion buffers and their use in culture studies. In R. A. Anderson (Ed.), *Algal culturing techniques* (pp. 35–65). Amsterdam, the Netherlands: Elsevier.

Sundquist, E. T., Plummer, L. N., & Wigley, T. M. L. (1979). Carbon-dioxide in the ocean surface-homogeneous buffer factor. *Science*, *204*, 1203–1205. https://doi.org/10.1126/science.204.4398.1203

Tarling, G. A., Peck, V., Ward, P., Ensor, N. S., Achterberg, E., Tynan, E., … Zubkov, M. V. (2016). Effects of acute ocean acidification on spatially-diverse polar pelagic foodwebs: Insights from on-deck microcosms. *Deep Sea Research II*, *127*, 75–92. https://doi.org/10.1016/j.dsr2.2016.02.008

Tatters, A. O., Roleda, M. Y., Schnetzer, A., Fu, F., Hurd, C. L., Boyd, P. W., … Hutchins, D. A. (2013). Short- and long-term conditioning of a temperate marine diatom community to acidification and warming. *Philosophical Transactions of the Royal Society B: Biological Sciences*, *368*, 1627.

Tatters, A. O., Schnetzer, A., Fu, F., Lie, A. Y. A., Caron, D. A., & Hutchins, D. A. (2013). Short-versus long-term responses to changing CO_2 in a coastal dinoflagellate bloom: Implications for interspecific competitive interactions and community structure. *Evolution*, *67*, 1879–1891. https://doi.org/10.1111/evo.12029

Taylor, A. R., Brownlee, C., & Wheeler, G. L. (2012). Proton channels in algae: Reasons to be excited. *Trends in Plant Science*, *17*, 675–684. https://doi.org/10.1016/j.tplants.2012.06.009

Trimborn, S., Brenneis, T., Hoppe, C. J. M., Laglera, L. M., Norman, L., Santos-Echeandía, J., … Hassler, C. S. (2017). Iron sources alter the response of Southern Ocean phytoplankton to ocean acidification. *Marine Ecology Progress Series*, *578*, 35–50. https://doi.org/10.3354/meps12250

Tynan, E., Clarke, J. S., Humphreys, M. P., Ribas-Ribas, M., Esposito, M., Rérolle, V. M. C., … Achterberg, E. P. (2016). Physical and biogeochemical controls on the variability in surface pH and calcium carbonate saturation states in the Atlantic sectors of the Arctic and Southern Oceans. *Deep Sea Research Part II*, *127*, 7–27. https://doi.org/10.1016/j.dsr2.2016.01.001

Welschmeyer, N. A. (1994). Fluorometric analysis of chlorophyll a in the presence of chlorophyll b and pheopigments. *Limnology and Oceanography*, *39*, 1985–1992. https://doi.org/10.4319/lo.1994.39.8.1985

Wolf-Gladrow, D. A., Bijma, J., & Zeebe, R. E. (1999). Model simulation of the carbonate chemistry in the microenvironment of symbiont bearing foraminifera. *Marine Chemistry*, *64*, 181–198. https://doi.org/10.1016/S0304-4203(98)00074-7

Wu, Y., Campbell, D. A., Irwin, A. J., Suggett, D. J., & Finkel, Z. V. (2014). Ocean acidification enhances the growth rate of larger diatoms. *Limnology and Oceanography*, *59*, 1027–1034. https://doi.org/10.4319/lo.2014.59.3.1027

Yool, A., Popova, E. E., Coward, A. C., Bernie, D., & Anderson, T. R. (2013). Climate change and ocean acidification impacts on lower trophic levels and the export of organic carbon to the deep ocean. *Biogeosciences*, *10*, 5831–5854. https://doi.org/10.5194/bg-10-5831-2013

Zeebe, R. E., Wolf-Gladrow, D. A., Bijma, J., & Hornisch, B. (2003). Vital effects in foraminifera do not compromise the use of δ11B as a paleo-pH indicator: Evidence from modelling. *Paleoceanography*, *18*, 1043.

SUPPORTING INFORMATION

Additional supporting information may be found online in the Supporting Information section at the end of the article.

How to cite this article: Richier S, Achterberg EP, Humphreys MP, et al. Geographical CO_2 sensitivity of phytoplankton correlates with ocean buffer capacity. *Glob Change Biol*. 2018;24:4438–4452. https://doi.org/10.1111/gcb.14324